

# Relationship Between Wear and Pitting Phenomena in Worm Gears

Michel Octrue

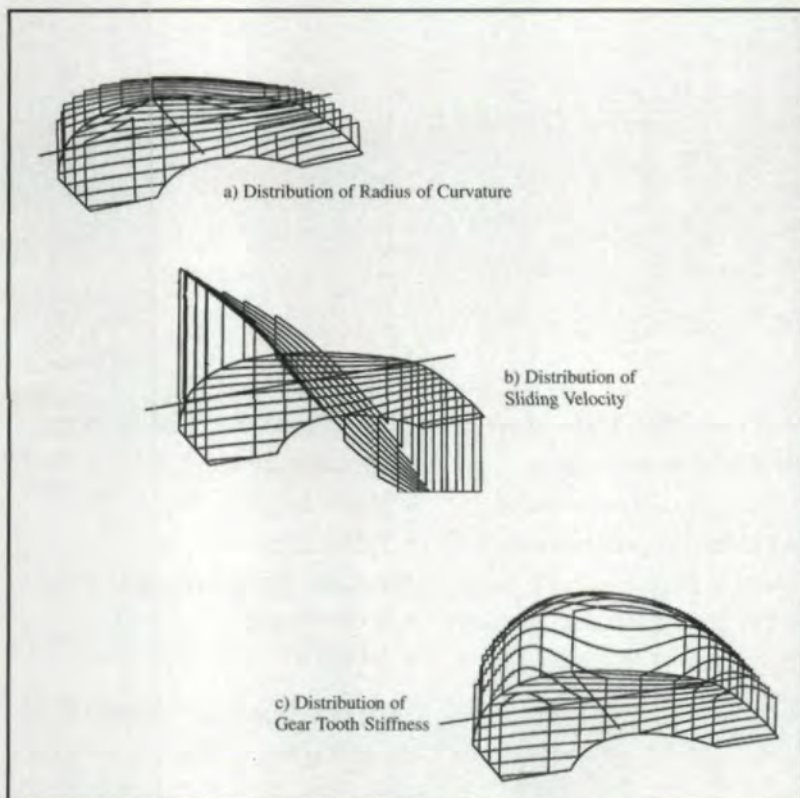


Fig. 1 — Physical parameters' distribution along lines of contact influencing wear phenomena in worm gears (Gear Ratio: 3/31).

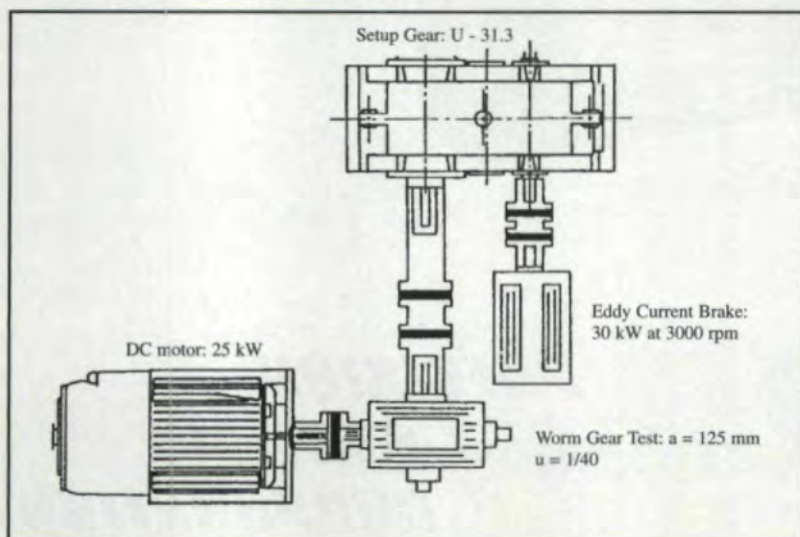


Fig. 2 — Worm gear test rig.

## Introduction

Worm gears display unique behavior of surfaces because of the presence of wear phenomena in addition to contact pressure phenomena.

**Physical Phenomena.** In worm gears the contact between the two surfaces of the teeth, the worm threads and the worm wheel teeth, evolves along lines of contact with a sliding velocity induced by the translation to the worm threads and the rotation of the worm wheel and the rotation of the worm. This last element provides the major component of sliding phenomena.

Consequently, unlike the case with cylindrical gears, it is difficult to separate the usual effects caused by contact pressure, which stresses the subsurface of teeth, and the wear effects caused by this important sliding phenomenon which stresses only the surfaces of the teeth.

**State of Calculation Methods.** Calculation methods or standards (Refs. 2-3) used for worm gears define two main criteria for rating: contact pressure or wear and tooth bending. Comparison of these criteria gives, in general, a torque limitation caused by pressure or wear.

The complexity of the geometry of worm gears has led to the establishment of empirical rating methods.

More recently, the use of computers has allowed a more theoretical approach, taking into account physical phenomena such as contact pressure and elastohydrodynamic lubrication induced in worm gear meshes. These methods are classified as **analytical**.

Nevertheless, the wear phenomena inherent in worm gears are still too complex to be approached by theory. This results in the different conditions of sliding velocity, radius of curvature and local stiffness encountered along the lines of contact between a worm and a worm wheel (Fig. 1). This is why it is necessary to characterize wear phenomena quantitatively according to experimental results and observations.

## Experimental Approach

For the last 12 years, CETIM has performed several endurance tests on worm gears. These tests were of long duration in order to reach a significant number of cycles of meshing on worm wheel teeth and to give pertinent data on the behavior of tooth surfaces.

To reach this goal, CETIM designed and developed three test rigs to test worm gear reducers.

**Test Rigs' Description.** Each test rig consists of a variable-speed, DC motor that drives the worm of the reducer to be tested with a torque meter. The worm wheel of the reducer is connected to an increaser that drives an eddy current brake used to apply the load. The brake is set up in balance in order to measure the applied torque (Fig. 2).

Each test rig is monitored, and the following parameters are measured continuously:

- Rotational speed of the worm,
- Torque on the input shaft of the worm,
- Applied torque on the output,
- Oil temperature in the sump,
- Oil temperature near the more heavily loaded worm bearing,
- The instantaneous wear of the worm gear.

The lubrication systems of worm gear reducers are composed of a pump, a heat exchanger cooled by water and a tank for oil. A water circulation bypass is used for temperature regulation of oil.

The configuration of the worm gear reducer is such that the worm is above the worm wheel. The oil inlet is above the worm near the more heavily loaded worm bearing and the outlet is at the bottom of the housing.

**Worm Gear Data.** Each test rig corresponds to a worm gear reducer.

### Testing Process

**Assembling:** The housing is cleaned, and the contact pattern of the worm gear is tracked with a soft blue dye slightly on the leaving side of the worm wheel and adjusted accordingly.

**Running in:** The lubricant system is filled with new oil, and the worm gear reducer is run at its nominal speed with a load increasing as follows:

- First hour: 10% of nominal torque
- Two hours: 25% of nominal torque
- Fifty hours: 50% of nominal torque

Then the oil is changed, the initial tooth backlash is measured in four positions of the worm wheel and the contact pattern is checked.

**Testing:** The torque is fixed at the test value, and each 300 hours the test rig is stopped. A sample of oil is taken for analysis just after stopping the test rig. The temperature of the worm gear

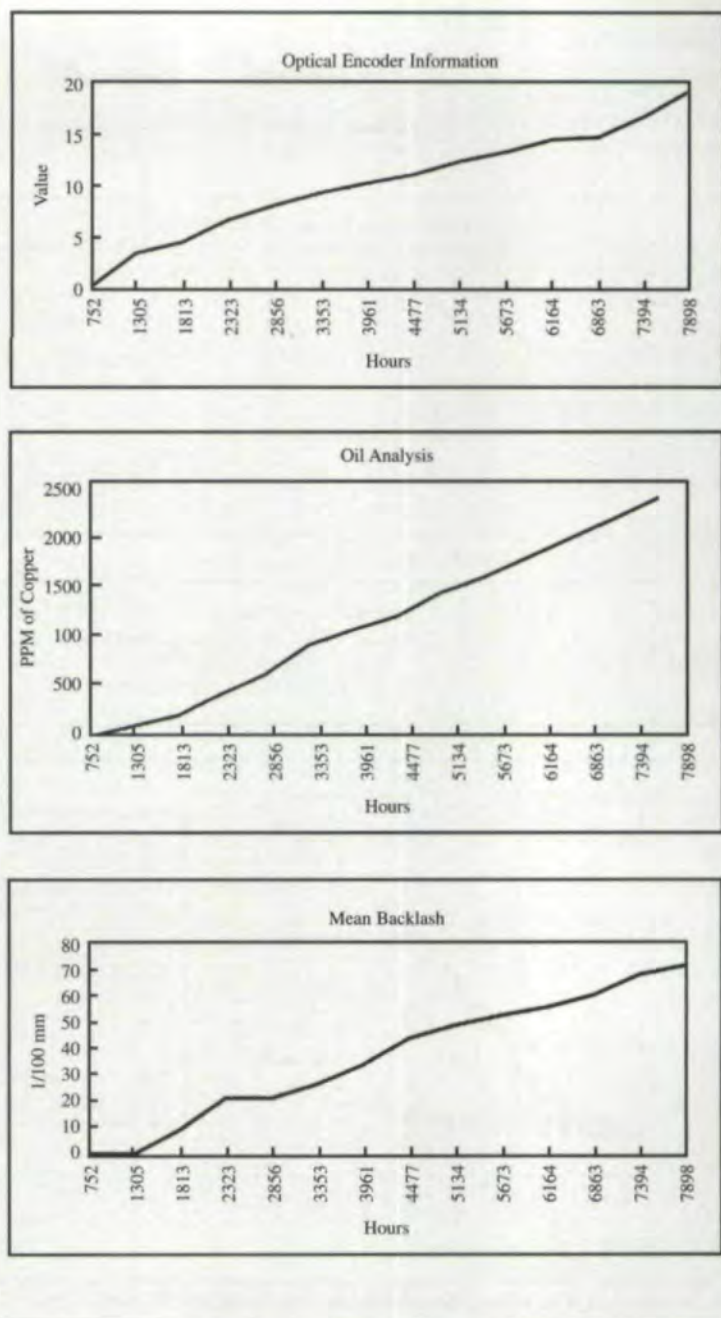


Fig. 3 — Comparison of wear measurement methods. reducer is decreased to ambient temperature. The level of oil is decreased so the worm wheel teeth are no longer in contact. The backlash is measured in four positions on the worm wheel, and the contact pattern is checked. The oil level is re-established, and the test rig is started again with a progressive loading in order to stabilize the temperature.

### Evaluation of Wear on Worm Wheels

Wear is determined by two direct measurements:

- A continuous measurement made using two optical encoders linked on each shaft of the worm and worm wheel and connected to a specific board that calculates the variation of the relative

### Dr. Michel Octrue

is manager of the gear department at the Centre Technique des Industries Mecaniques (CETIM) in Senlis, France. He is also the technical manager of the Institute de l'Engrenage et des Transmissions (IET) and president of the Technical Committee at EUROTRANS. He is the author of numerous books and papers on gearing subjects.

**Table I — Characteristics of Worm Gear Test Rigs**

		A	B	C
Nominal Input Power	[kW]	5.5	18	31
Nominal of Input Velocity	[rpm]	1500	1500	1500
Maximum Input Power	[kW]	15	37	64
Min/Max Input Velocity	[rpm]	1600	1500	1500
Max Output Torque	[daN.m]	3000	2500	2000

**Table II — Geometrical Data of Worm Gears**

		A	B	C
Center Distance	[mm]	125	125	125
Gear Ratio $u = z_1/z_2$		1/40	3/31	5/24
Axial Module	[mm]	4.95	6.45	8.36
Lead Angle [°]		5.4375	21.1369	40.2592
Normal Pressure Angle [°]		21.81	20.65	25
Worm Profile		A	A	A
Worm Wheel Face Width	[mm]	45	45	45
External Diameter of Worm Wheel	[mm]	220	220	220

**Table III— Materials and Lubricant**

Worm Material	Case-Hardened Steel
Worm Wheel	Bronze with 12% of tin and x% of nickel
Lubricant	Synthetic Oil: Polyglycol Shell TIVELA A — 150 Cst at 40°C

position of the worm for a defined space of the worm wheel teeth.

• A second measurement with the evaluation of backlash is made in four positions of the worm wheel at each stop of the test rig.

The last method takes into account the fact that the wear is not always a uniform phenomenon distributed on all worm wheel teeth. A mean value is deduced from the four measurements. (Note: In this article, the wear phenomena are discussed on the mean values.)

An indirect measurement of wear can also be obtained by the evaluation of the number of copper particles contained in the oil. This is obtained by the parts per million evaluated by oil analysis.

A comparison of these three methods is given in Fig. 3.

**Results of Wear Measurement**

Figs. 4–7 represent the evolution of wear interpreted as an increase of backlash. Only the variations of backlash are represented. Each curve corresponds to a specific working condition in terms of speed of the worm  $n_1$  and torque applied on the worm wheel  $C_2$ .

For a 1/40 ratio, two graphs are plotted, one in functions of the duration of test; the second in functions of the number of cycles applied on the worm gear teeth (Figs. 4–5).

The representation in functions of the number of cycles gives a better coherence between the different working conditions. This is true for all ratios.

The observations of these curves show that for all loading conditions, a period of meshing exists during which no wear appears. It corresponds to the time it takes for the surfaces to adapt. Then the increase of backlash begins and evolves continuously.

This evolution is not really linear except for the 5/24 ratio; more often it evolves like stairs, and after the initiation of the phenomenon, there are periods of greater or lesser stability separated by periods during which wear evolves continuously.

**Comparison With Predicted Results**

The comparisons are done according to DIN 3996 standards. This standard proposes a calculation method to predict the evolution of backlash as a function of the duration of working.

These calculations have been done for each worm gear and for two working conditions (Figs. 8–10). (In these figures, the first number between brackets represents the rotational speed of the worm in rpm and the second, the applied torque on the worm wheel in mN.) The first observation is that the wear prediction in DIN 3996 is a linear function. The sensitivity of DIN 3996 is the same

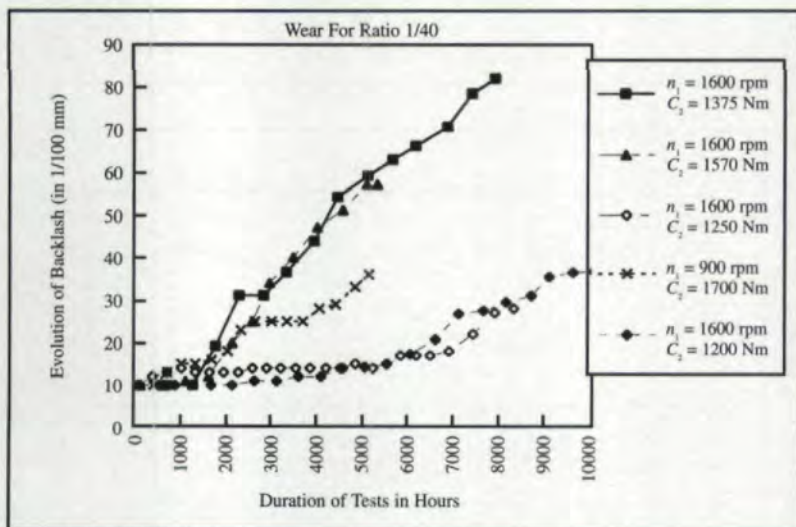


**Fig. 4 — Evolution of wear for ratio 1/40 in function of number of hours.**

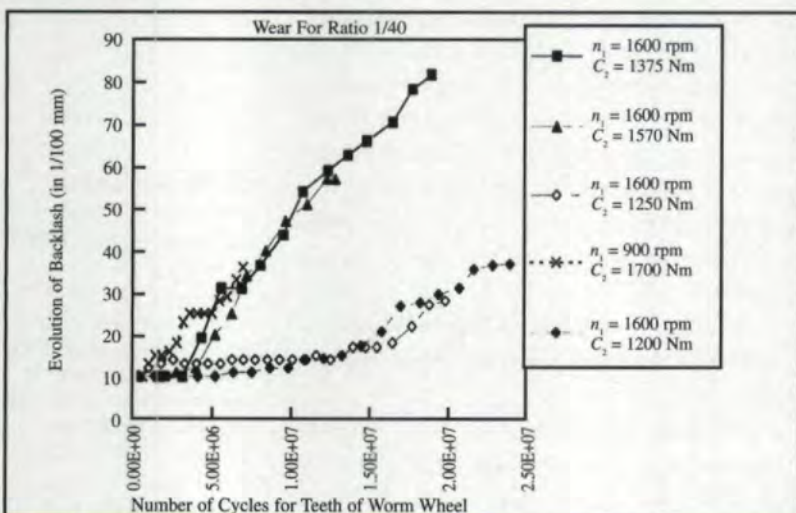


**Fig. 5 — Evolution of wear for ratio 1/40 in function of number of cycles.**

as for the experimental observations: If the torque increases, the wear increases. From the point of view of amplitude, theoretical predictions of wear and experimental results are not correlated: DIN 3996 predicts more wear for the ratio 1/40 than for the ratio 5/24. The experiment's observations show the contrary result.

### Observations & Predictions

In order to explain these differences, qualitative observations of the evolution of flanks during working were made. The following pictures present the evolution of the same tooth flank during the testing process.

Figs. 11–21 represent the behavior of the surface of the worm wheel:

- Figs. 11–14 for 1/40 ratio during 7900 hours.
- Figs. 15–19 for 3/31 ratio during 8000 hours.
- Figs. 20–21 for 5/24 ratio during 1460 hours.

These figures show the progressive process of wear and pitting phenomena. These two physical types of flank deterioration are merged together.

The theoretical contact pressure distributions, determined with the analytical calculation method developed at CETIM (Ref. 5), are represented in Figs. 22–24.

If there is a uniform contact pressure distribution, as in the case of one-start worms, the propagation of cracks is low; otherwise the propagation is more localized near the high pressure of contact induced by low radius of curvature.

In all cases, it can be observed that the localization of the maximum of the theoretical prediction of the contact pressure distribution is well correlated with the zones where cracks appear. Consequently, in worm gears, the contact pressure distribution is not uniform along the lines of contact.

### Interpretation of Phenomena

The first step of the process is linked to contact pressure and the induced cold working in the sublayer of surface where the maximum shear stress generally appears. Cracks are growing up under the surface near a depth close to 0.8 times the semi-width of contact. This depth is between 0.3 and 0.5 mm.

Cracks propagate more or less quickly toward the surface of the flanks as a function of the contact pressure level and the distribution of radius of curvature. When cracks have reached the surface, scales are removed, leaving small holes.

The transmitted load is redistributed on the part of the flank surface which is not scaled yet, and a new contact pressure distribution is established. This phenomenon evolves continuously up to the subsurface: Cracks have developed and reached the surface. An equivalent wear phenomenon on

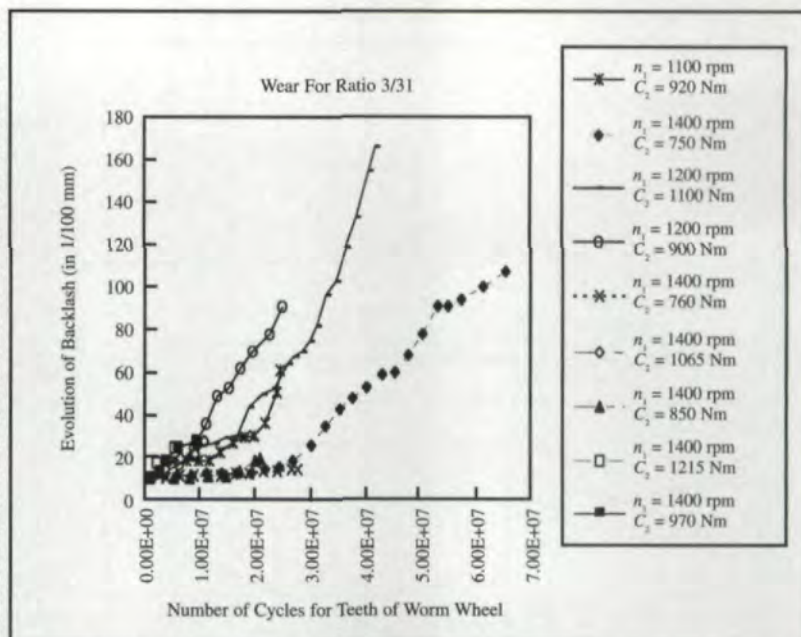


Fig. 6 — Evolution of wear for ratio 3/31 in function of number of cycles.

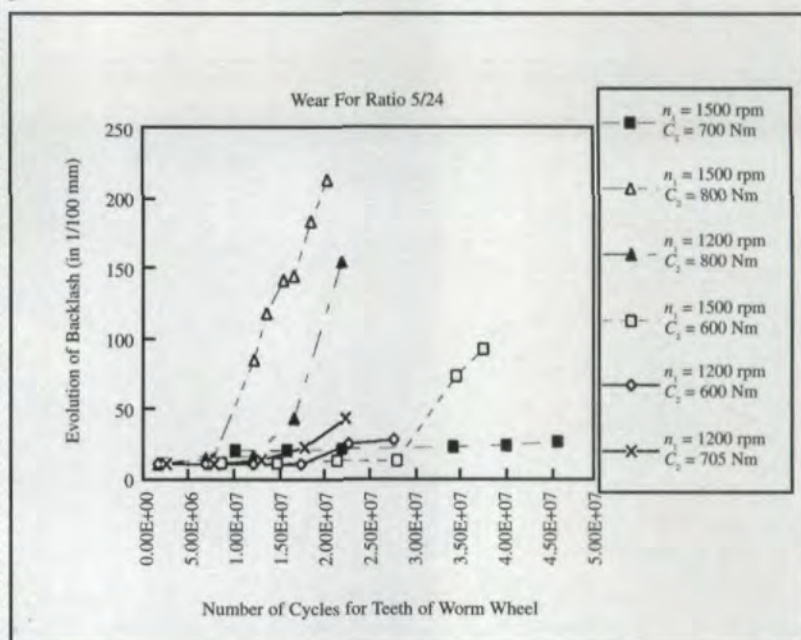


Fig. 7 — Evolution of wear for ratio 5/24 in function of number of cycles.

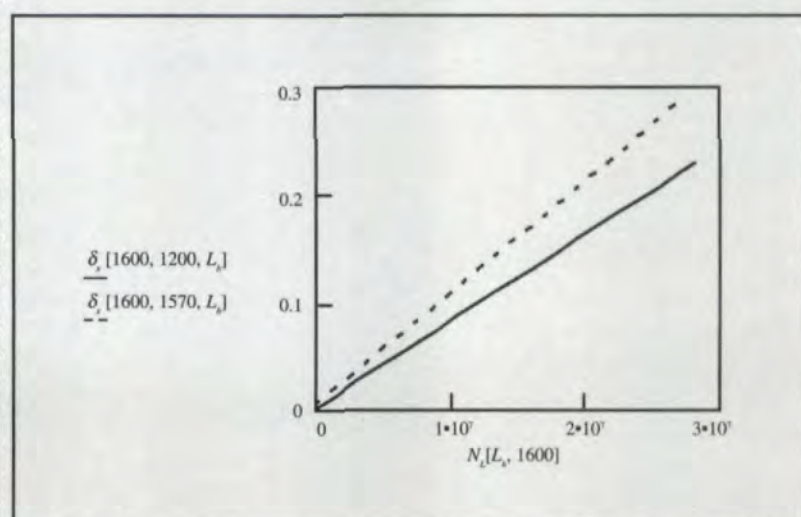


Fig. 8 — Prediction of wear by DIN 3996 for ratio 1/40 in function of number of cycles.

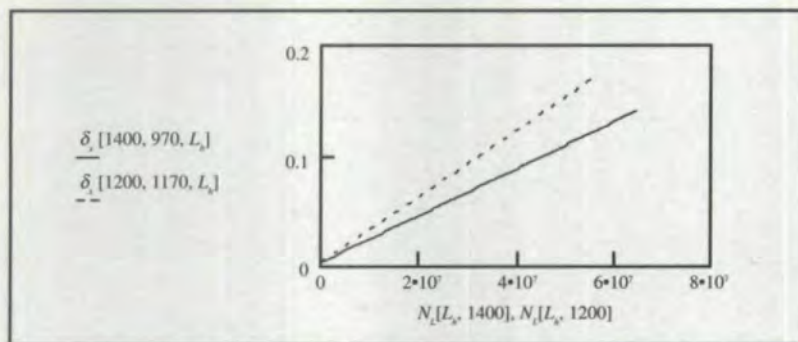


Fig. 9 — Prediction of wear by DIN 3996 for ratio 3/31 in function of number of cycles.

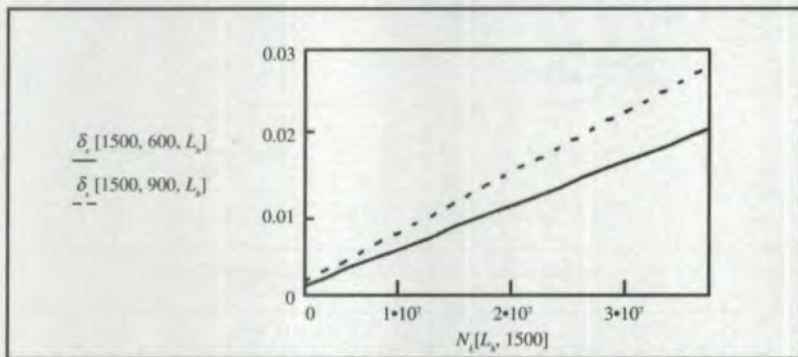


Fig. 10 — Prediction of wear by DIN 3996 for ratio 5/24 in function of number of cycles.



Fig. 11 — Worm gear 1/40:  $n_1 = 1600$  rpm;  $C_2 = 1374$  Nm after 2323 hours.

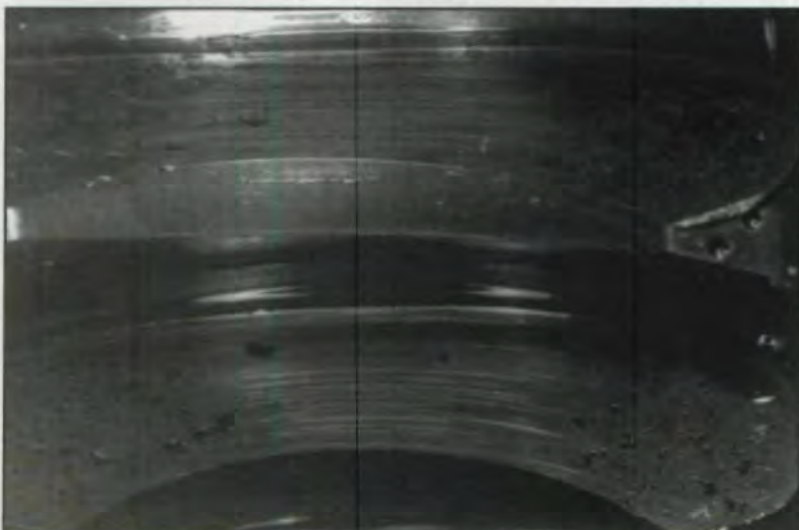


Fig. 12 — Worm gear 1/40:  $n_1 = 1600$  rpm;  $C_2 = 1374$  Nm after 4477 hours.

teeth is produced because material is removed, but the physical basis here is contact pressure.

The intensity of this phenomenon is directly linked to the radius curvature distribution of the worm gear. If this distribution is regular, as in one-start worm gears, the equivalent wear phenomenon will propagate slowly, and the resulting level of wear will be low.

When the pressure distribution is not regular, as in the case of 3- or 5-start worm gears, the equivalent wear phenomenon grows quickly, and the resulting wear level is high. This is observed in Figs. 5-7. In these cases, the heterogeneity of the worm wheel material can produce a non-homogeneity of tooth-to-tooth wear, thereby inducing pitch errors during working. These pitch errors can create internal dynamic effects caused by the bad load sharing between teeth, increasing the propagation of the equivalent wear phenomenon and, sometimes, the production of chocks during meshing.

#### A New Approach

In order to have a better prediction of worm gear life, it is necessary to have an approach based on the observed behavior of worm wheel flanks during working.

Our observations, described above, have shown that pressure contact phenomena are the basis of this kind of prediction. This implies the need to have a good knowledge of how the worm wheel is affected by contact pressure fatigue. To answer to this first question, CETIM has developed experimental investigations to determine S-N curves for several bronzes on roller-disk machines (Ref. 6).

In another way CETIM has developed an analytical method to determine contact pressure distribution, taking into account geometry (radius of curvature), kinematics (sliding velocity) and elasticity (gear tooth stiffness).

By coupling S-N curves with contact pressure distribution calculations, it is possible to predict the zones of tooth flanks on which scales will appear.

Then the calculation of removed surfaces can be made, and a new contact pressure distribution can be established. Taking into account the cumulative damages with S-N curves, the life of each point of flank surface can be predicted as the quantity of removed material and the equivalent wear phenomena.

This calculation has to be done iteratively: The contact pressure distribution is adjusted at each step, taking into account the leaving surface on worm wheel flanks. The surface strongly stressed is then removed, taking into account the contact

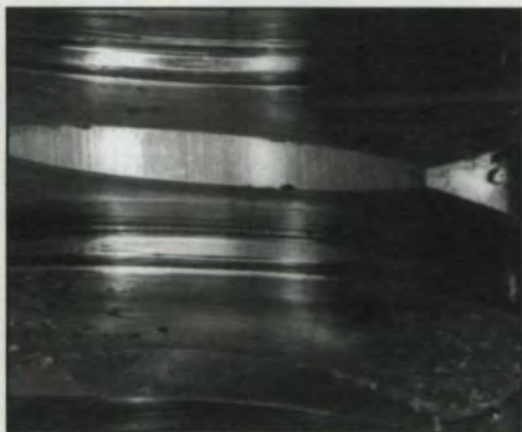


Fig. 13 — Worm gear 1/40:  $n_1 = 1600$  rpm;  $C_2 = 1374$  Nm after 6863 hours.

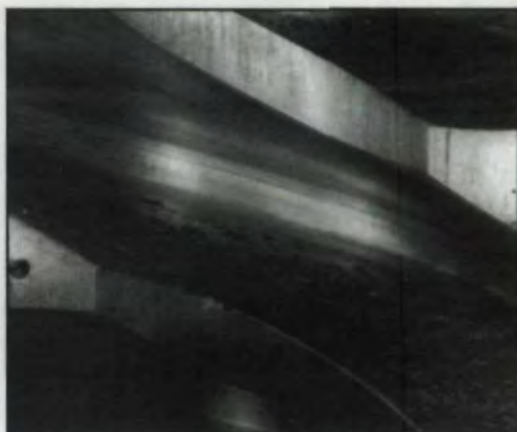


Fig. 17 — Worm gear 3/31:  $n_1 = 1400$  rpm;  $C_2 = 750$  Nm after 4032 hours.

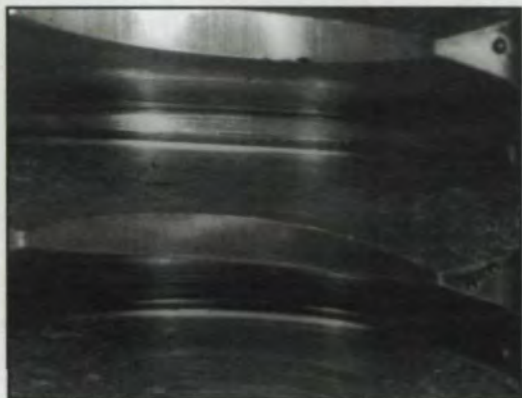


Fig. 14 — Worm gear 1/40:  $n_1 = 1600$  rpm;  $C_2 = 1374$  Nm after 7898 hours.

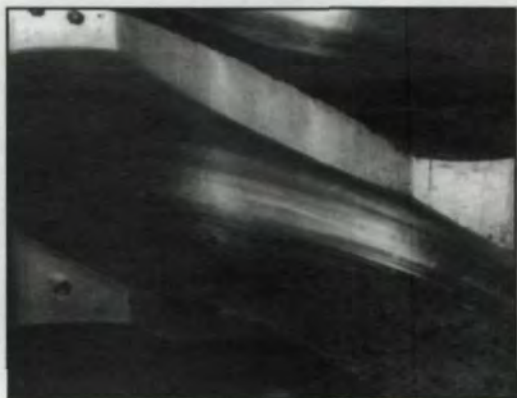


Fig. 18 — Worm gear 3/31:  $n_1 = 1400$  rpm;  $C_2 = 750$  Nm after 5292 hours.

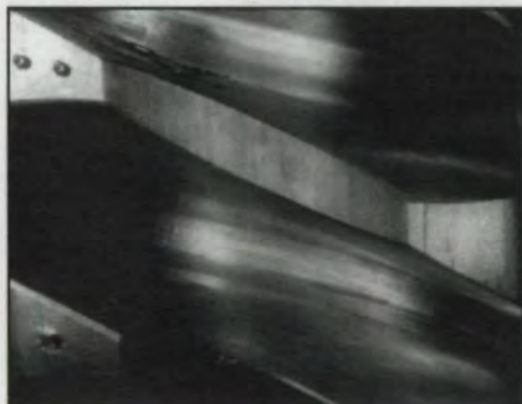


Fig. 15 — Worm gear 3/31:  $n_1 = 1400$  rpm;  $C_2 = 750$  Nm after 735 hours.



Fig. 19 — Worm gear 3/31:  $n_1 = 1400$  rpm;  $C_2 = 750$  Nm after 8033 hours.



Fig. 16 — Worm gear 3/31:  $n_1 = 1400$  rpm;  $C_2 = 750$  Nm after 3302 hours.

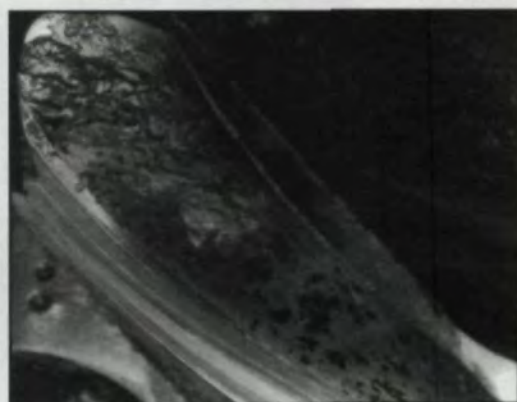


Fig. 20 — Worm gear 5/24:  $n_1 = 1200$  rpm;  $C_2 = 800$  Nm after 1113 hours.

FOR ALL  
LOADING  
CONDITIONS,  
A PERIOD OF  
MESHING,  
CORRESPONDING  
TO THE TIME IT  
TAKES SURFACES  
TO ADAPT,  
EXISTS DURING  
WHICH NO  
WEAR APPEARS.  
THEN BACKLASH  
BEGINS AND  
EVOLVES  
CONTINUOUSLY.



Fig. 21 — Worm gear 5/24:  $n_1 = 1200$  rpm;  $C_2 = 800$  Nm after 1463 hours.

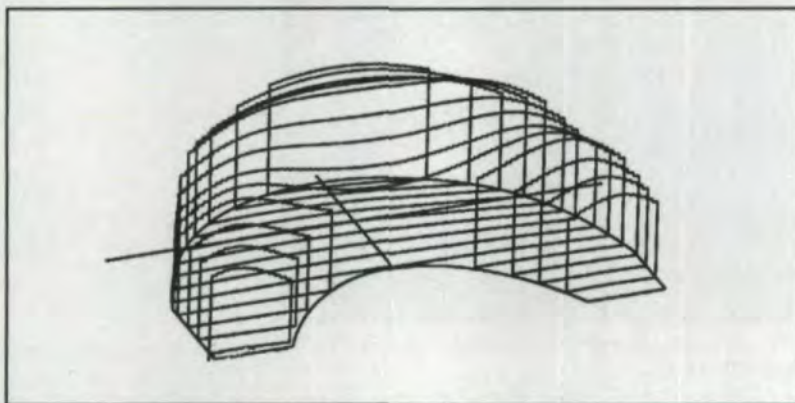


Fig. 22 — Pressure distribution on worm wheel flank for worm gear 1/40.

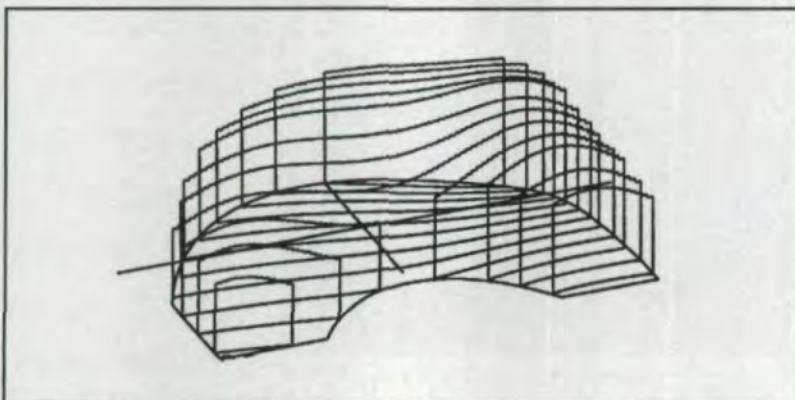


Fig. 23 — Pressure distribution on worm wheel flank for worm gear 3/31.

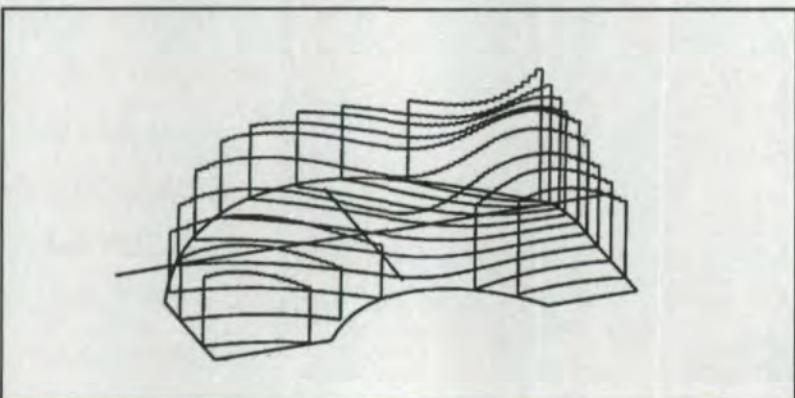


Fig. 24 — Pressure distribution on worm wheel flank for worm gear 5/24.

pressure S-N curve the material. A new leaving surface on the worm wheel flanks is determined for the next step of the calculation.

### Conclusions

Experimental results presented in this paper, based on more than 50,000 hours of tests on real worm gear sets, provide a basis to evaluate wear phenomena.

It has been clearly established that analysis of the percentage of copper in the lubricating oil provides a good clue to the wear rate of worm gears. We also learned that:

- Wear phenomena are not a continuous effect starting as soon as the worm gear is running. A period of incubation is necessary during which contact pressure phenomena initiate cracks through the subsurfaces of the tooth flanks. When these cracks reach the surface, scaling appears, and an equivalent wear phenomenon appears which reflects a balance between weakness of material near the surface and redistribution of transmitted load on the surface.
- The second observation is that for worm gears, the contact pressure distribution is never constant on tooth flanks. The proposed analytical approach correlates well with observations.

The complexity of these fatigue surface phenomena have led us to propose a new approach in order to be able to predict surface durability of worm gears. It will be based on contact pressure. ☉

### References:

1. AGMA Standard 6022-C93. "Design Manual for Cylindrical Worm Gearing."
2. AGMA Standard 6034-B92. "Practice for Enclosed Cylindrical Worm Gears, Speed Reducers and Gearmotors."
3. BS 721-1963/Confirmed 1984. "Specification for Worm Gearing."
4. DIN 3996-1996. "Calculation of Load Capacity of Cylindrical Worm Gear Pairs With Shaft Angle  $\Sigma = 90^\circ$ ."
5. Octrue, M. "A New Method of Designing Worm Gears." AGMA FTM, 1988.
6. Octrue, M. & M. Guingand. "Experimental Characterization of Surface Durability of Materials for Worm Gears." AGMA FTM 1992.

**Acknowledgement:** First presented at the AGMA Fall Technical Meeting, November 9-11, 1997, San Diego, CA. 97FTM9. ©AGMA, 1997. Reprinted with permission.

### Tell Us What You Think . . .

If you found this article of interest and/or useful, please circle 210.

For more information about CETIM, please circle 211.